In Proceedings of Graphed-based Representation Workshop GbR 2003, York.

Constructing Stochastic Pyramids by MIDES - Maximal Independent Directed Edge Set *

Yll Haxhimusa[1] and Roland Glantz[2] and Walter G. Kropatsch[1]

[1] Pattern Recognition and Image Processing Group 183/2
Institute for Computer Aided Automation
Vienna University of Technology
Favoritenstrasse 9, A-1040 Vienna, Austria
{yll, krw}@prip.tuwien.ac.at
[2] Dipartimento di Informatica
Università di Ca' Foscari di Venezia
Via Torino 155, 30172 Mestre (VE), Italy
glantz@dsi.unive.it

Abstract. We present a new method (MIDES) to determine contraction kernels for the construction of graph pyramids. Experimentally the new method has a reduction factor higher than 2.0. Thus, the new method yields a higher reduction factor than the stochastic decimation algorithm (MIS) and maximal independent edge set (MIES), in all tests. This means the number of vertices in the subgraph induced by any set of contractible edges is reduced to half or less by a single parallel contraction. The lower bound of the reduction factor becomes crucial with large images.

Keywords: irregular graph pyramids, maximal independent set, maximal independent directed edge set, topology preserving contraction.

1 Introduction

In a regular image pyramid the number of pixels at any level k, is λ times higher than the number of pixels at the next reduced level $k+1$. The so called reduction factor λ is larger than 1 and it is the same for all levels k. If P denotes the number of pixels in an image I, the number of new levels on top of I amounts to $log_\lambda(P)$ (Figure 1(a)). Thus, the regular image pyramid may be an efficient structure to access image objects in a top-down process. For more in depth on the subject see [20].

However, regular image pyramids are confined to globally defined sampling grids and lack shift invariance [1]. In [19, 10] it was shown how these drawbacks can be avoided by irregular image pyramids, the so called adaptive pyramids, where the hierarchical structure (vertical network) of the pyramid was not a priori known but recursively built based on the data. Moreover in [18, 4, 16, 2] it

* This paper has been supported by the Austrian Science Fund under grants P14445-MAT and P14662-INF

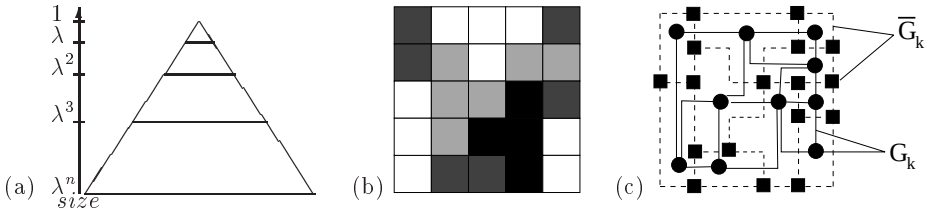

Fig. 1. (a) Pyramid concept. (b) Partition of pixel set into cells. (c) Representation of the cells and their neighborhood relations by a dual pair $(G, \overline{G})$ of plane graphs.

was shown that the irregular pyramid can be used for segmentation and feature detection.

Each level represents a partition of the pixel set into cells, i.e. 4-connected subsets of pixels. The construction of an irregular image pyramid is iteratively local [17, 9]:

- the cells have no information about their global position.
- the cells are connected only to (direct) neighbors.
- the cells cannot distinguish the spatial positions of the neighbors.

On the base level (level 0) of an irregular image pyramid the cells represent single pixels and the neighborhood of the cells is defined by the 4-connectivity of the pixels. A cell on level $k+1$ (parent) is the union of some neighboring cells on level k (children). This union is controlled by so called contraction kernels (decimation parameters [13]). For more in depth on the subject see the book of Jolion [11]. Neighborhoods on level $k+1$, are derived from neighborhoods on level k. Two cells c_1 and c_2 on level $k+1$ are neighbors if there exist children p_1 of c_1 and p_2 of c_2 such that p_1 and p_2 are neighbors in level k, Figure 1(b). We assume that on each level $l+1$ ($l \geq 0$) there exists at least one cell not contained in level l. In particular, there exists a highest level h . Furthermore, we restrict ourselves to irregular pyramids with an apex, i.e. level h contains one cell.

In this paper we represent the levels as dual pairs $(G_k, \overline{G_k})$ of plane graphs G_k and $\overline{G_k}$, Figure 1(c). The vertices of G_k represent the cells and the edges of G_k represent the neighborhood relations of the cells on level k, depicted with circle vertices and solid edges in Figure 1(c). The edges of $\overline{G_k}$ represent the borders of the cells on level k, depicted with dashed lines in Figure 1(c), possibly including so called pseudo edges needed to represent the neighborhood relation to a cell completely surrounded by another cell. Finally, the vertices of $\overline{G_k}$, the squares in Figure 1(c), represent points where at least three edges from $\overline{G_k}$ meet. The sequence $(G_k, \overline{G_k})$, $0 \leq k \leq h$ is called (dual) graph pyramid.

The homogeneous region does not offer additional information to be used to contract this region. Thus the stochastic selection principle is used to contract a homogeneous region. The aim of this paper is to combine the advantage of regular pyramids (logarithmic tapering) with the advantages of irregular graph pyramids (their purely local construction and shift invariance). The aim is reached by ex-

changing the stochastic selection method (MIS) for contraction kernels proposed in [17] by another iteratively local method (MIDES) that has a reduction factor higher than 2.0 in all out experiments. The other goal is not to be limited by the direction of contraction, which is a drawback of MIES [7]. Experiments with both selection methods show that:

- the MIS method does not lead necessarily to logarithmic tapering graph pyramids, i.e. the reduction factors of graph pyramids built by the MIS can get arbitrarily close to 1.0 [19].
- the sizes of the receptive fields from the new method (MIDES) are much more uniform.

Not only stochastic decimation [17], but also connected component analysis [15] gains from the new method.

The plan of the paper is as follows. In Section 2 we recall the main idea of the stochastic pyramid algorithm and in Section 2.3 we see that graph pyramids from maximal independent vertex sets (MIS) may have a very small reduction factor. Moreover, experiments show that small reduction factors are likely, especially when the images are large. We propose a new method (MIDES), in Section 3, based on directed graphs and show in Section 3.2 that this method has a reduction factor larger than 2.0.

2 Maximal Independent Vertex Set

In the following the iterated stochastic construction of the irregular image pyramid in [17, 4, 16] is described in the language of graph pyramids. The main idea is to first calculate a so called *maximal independent vertex set*[1] [5]. Let V_k and E_k denote the vertex set and the edge set of G_k, respectively and let $\iota(\cdot)$ be the mapping from an edge to its set of end vertices. The neighborhood $\Gamma_k(v)$ of a vertex $v \in V_k$ is defined by

$$\Gamma_k(v) = \{v\} \cup \{w \in V_k \mid \exists e \in E_k \text{ such that } v, w \in \iota(e)\}.$$

A subset W_k of V_k is called maximal independent vertex set if:

1. $w_1 \notin \Gamma_k(w_2)$ for all $w_1 \neq w_2 \in W_k$,
2. for all $v \in V_k \setminus W_k$ there exists $w \in W_k$ such that $v \in \Gamma_k(w)$.

Put in words, two members (survivors) of maximal independent vertex set cannot be neighbors (condition 1) and every non-member (non-survivor) is in the neighborhood of at least one member (condition 2). An example of a maximal independent vertex set is shown with black vertices in Figure 2(a), the arrows indicate a corresponding collection of contraction kernels.

[1] also called maximal stable set; we distinguish maximal from maximum independent set, whose construction is NP-complete. See [5] for algorithmic complexity.

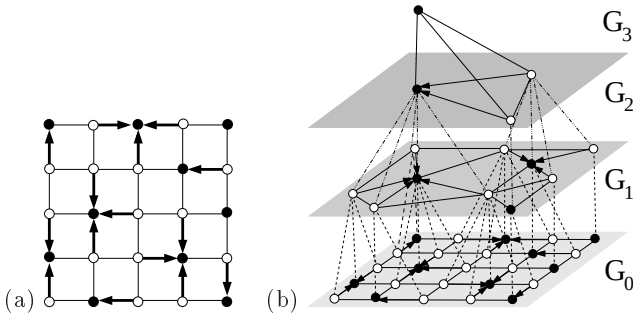

Fig. 2. (a) Maximal independent vertex set. (b) A graph pyramid from maximal independent vertex set.

2.1 Maximal Independent Vertex Set Algorithm (MIS)

The maximal independent vertex set (MIS) problem was solved using parallel, probabilistic symmetry breaking algorithm [17]. The number of iterations to complete maximal independent set converges in most of the cases very fast, only few iterations for correction are needed [17] .

MIS may be generated as follows.

Algorithm 1 – MIS Algorithm

1: Mark every vertex v of V_l as *candidate*.
2: **while** there are candidates **do**
3: Assign random numbers to the candidates of V_l.
4: Determine the candidates whose random numbers are larger than the random numbers of all neighboring candidates and mark them as *member* (of the maximal independent set) and as *non-candidate*. Also mark every neighbor of every new member as *non-candidate* and as *non-member*.
5: **end while**
6: In each neighborhood of a vertex that is not a member there will now be a member. Let each non-member choose its neighboring member, say the one with the maximal random number (we assume that no two random numbers are equal).

The assignment of the non-members to their members determines a collection of *contraction kernels*: each non-member is contracted toward its member and all contractions can be done in a single parallel step. In Figure 2(a) the contractions are indicated by arrows. A stochastic graph pyramid with MIS can be seen in Figure 2(b), where $G_0, G_1, ...$ etc. represent graphs on different levels of the pyramid. Note that we remove parallel edges and self-loops that emerge from the contractions, if they are not needed to encode inclusion of regions by other regions (in the example of Figure 2(b) we do not need loops nor parallel edges). This can be done by the dual graph contraction algorithm [13].

2.2 Experimental Setup and Evaluation

Uniformly distributed random numbers are assigned to vertices or edges in the base grid graphs. We generated 1000 graphs, on top of which we build stochastic graph pyramids. In our experiments we use graphs of sizes 10000 and 40000 nodes, which correspond to image sizes 100×100 and 200×200 pixels, respectively. Figure 3 summarizes the result of the first 100 of 1000 tests. Data in Table 1 and Table 2 were derived using graphs of size 200×200 nodes with 1000 experiments.

We extract the following parameters: the height of the pyramid (*height*); the maximum and the mean of the degree of vertices [2] (*max-degree* and *mean-degree*); and the number of iterations for correction (*correction*) to complete maximal independent set for any graph in the contraction process (Table 1). In Table 2 are shown reduction factors for vertices ($|V_k|/|V_{k+1}|$) and edges ($|E_k|/|E_{k+1}|$). We average these values on the whole data set (μ-mean and σ-standard deviation). The degree of the vertex is of importance because it is directly related to the memory costs for the graph's representation [9]. We compare the quality of selection methods in Section 2.3 and 3.2. A full documentation of the experiments can be found in the technical report [8].

2.3 Experiments with MIS

The number of levels needed to reduce the graph at the base level (level 0) to an apex (top of the pyramid) are given in Figure 3(a),(b). The vertical axis indicates the number of nodes on the levels indicated by the horizontal axis. The slopes of the lines correspond to the reduction factors. From Figure 3(a),(b) we see that the **height** of the pyramid **cannot be guaranteed to be logarithmic**, except for some good cases.

In the worst case the pyramid had 22 levels for the 100×100, respectively 41 levels for the 200×200 graphs. See [8] for numerical details. In these cases we have a very poor reduction factor. A **poor reduction factor** is likely, as can be seen in Figure 3(a),(b), especially when the **images are large**. This is due to the evolution of larger and larger variations between the vertex degrees in the contracted graphs (Table 1 *max-degree* and *mean-degree* columns). The absolute maximum vertex degree was 148. The *a priori* probability of a vertex being the local maximum dependents on its neighborhood. The larger the neighborhood the smaller is the *a priori* probability that a vertex will survive. The number of iterations necessary for correction are the same as reported by [17] (Table 1 *correction* columns).

To summarize, a **constant reduction factor cannot be guaranteed**.

[2] the number of edges incident to a vertex, i.e the number of non survivor contracted into the survivor.

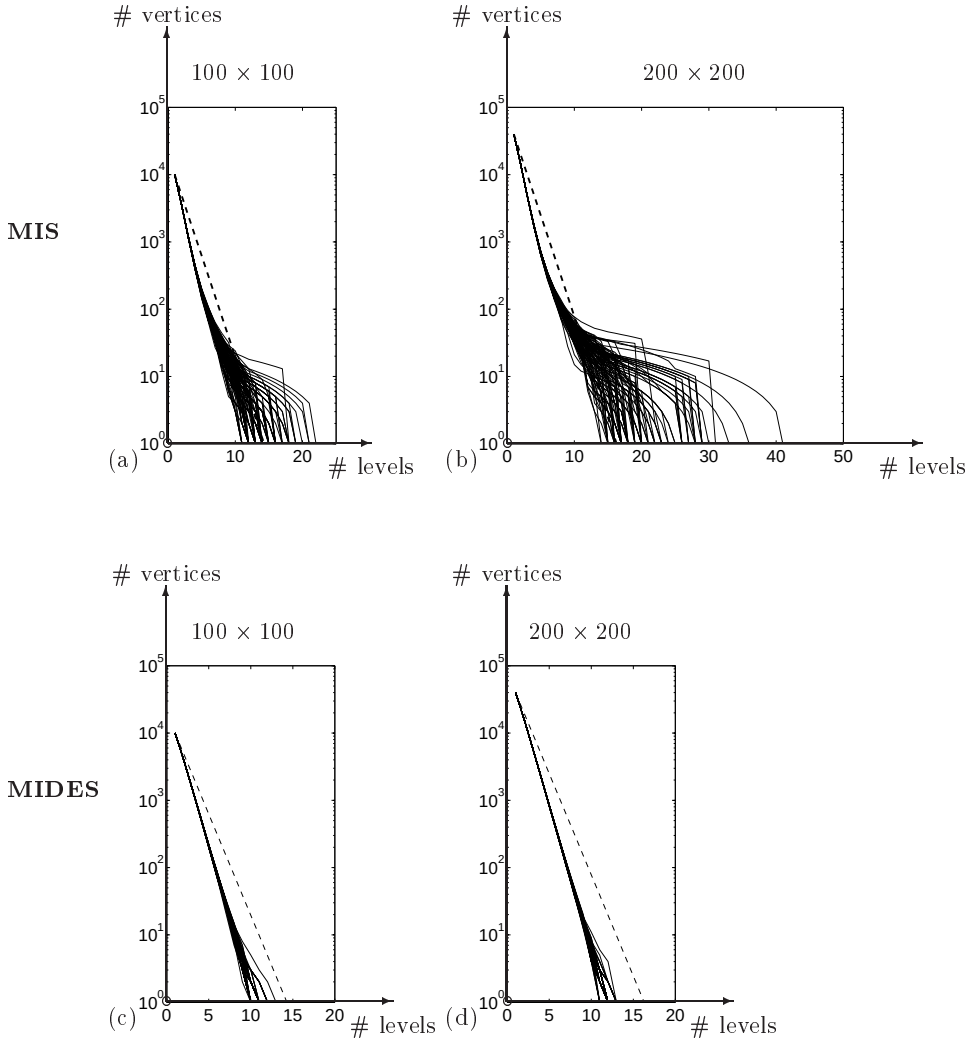

Fig. 3. Comparing MIS and MIDES. Number of vertices in levels of MIS and MIDES pyramids. The base levels are rectangular grid graphs containing 100×100 and 200×200 vertices . Dashed lines represent the theoretical reduction factor of 2.0 (MIES [7]).

Table 1. Comparison of MIS,MIES and MIDES.

Process	*height*		*max-degree*		*mean-degree*		*correction*	
	μ	σ	μ	σ	μ	σ	μ	σ
MIS	20.78	5.13	70.69	23.88	4.84	0.23	2.95	0.81
MIES	14.01	0.10	11.74	0.71	4.78	0.07	4.06	1.17
MIDES	12.07	0.46	13.29	1.06	4.68	0.14	2.82	1.07

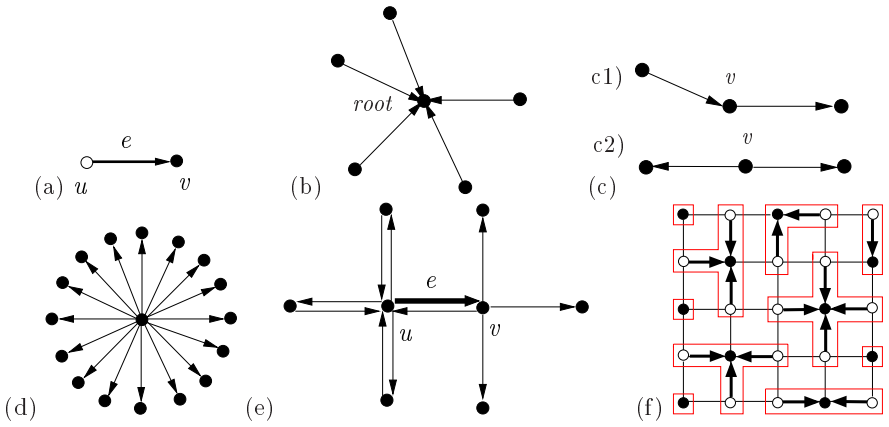

Fig. 4. (a) The direction of contraction. (b) A legal configuration of directed edges. (c) Forbidden pairs of directed edges. (d) The reduction factor of a star with n edges pointing away from the center is $n/(n-1)$. (e) The directed neighborhood $N(e)$. (f) Maximal independent directed edge set with respect to $N(e)$.

3 Maximal Independent Directed Edge Set

In many graph pyramid applications such as line image analysis [3,14], the description of image structure [6,12], a directed edge e with source u and target $v \neq u$ must be contracted (from u to v, Figure 4(a)), only if the attributes of e, u, and v fulfill a certain condition, making the direction of contraction an important issue. In line drawings end point of lines or intersection must be preserved for geometric accuracy reasons. In particular, the condition depends on u being the source and v being the target. The edges that fulfill the condition are called *preselected* edges.

From now on the plane graphs in the pyramid have (bi)directed edges. Typically, the edges in the base level of the pyramid form pairs of reverse edges, i.e. for each edge e with source u and target v there exists an edge e' with source v and target u. However, the set of preselected edges may contain e without containing e'. The goal is to build contraction kernels with a "high" reduction factor from the set of preselected edges, such that a predetermined target v survives. The reduction will always be determined according to the directed graph induced by the preselected edges. For example, if the number of vertices in the induced subgraph is reduced to half, the reduction factor will be 2.0. To perform the contractions in parallel, we need a vertex disjoint union of contraction kernels. The plan is to define such a union in terms of independent directed edges, where "independent" means that no pair of directed edges belongs to the same neighborhood $N(e)$ (see Definition 3). Then, dealing with edges instead of vertices, we may find the contraction kernels as in MIS.

Definition 1. *A contraction kernel is a vertex disjoint rooted tree of depth one or zero (single vertex), each edge of which is directed toward the root (survivor).*

Note that the direction of edges uniquely determines which vertex survives on the next level of the pyramid, i.e determines the contraction kernel (decimation parameter [13]). Figure 4(b) shows a configuration of directed edges, which yields a contraction kernel.

Definition 2. *Let v be a vertex of bi-directed graph G. We define the out-degree as*

$$s(v) := \#\{e \in G \mid v \text{ is source of } e\},$$

and in-degree as

$$t(v) := \#\{e \in G \mid v \text{ is target of } e\}.$$

In Figure 4(b) the number of edges with target in *root* is $t(root) = 5$; and for the center vertex with n edges pointing away $s(center) = n$, Figure 4(d).

Proposition 1. *Let D denote a set of directed edges from a bi-directed graph G and G_D denote the subgraph induced by D. Then the following statements are equivalent:*

(a) $s(v) < 2 \ \wedge \ s(v) \cdot t(v) = 0, \quad \forall v \in G_D$.
(b) *G_D is a vertex disjoint union of contraction kernels.*

Proof. **i)** (a) $\Rightarrow$ (b): Let $R := \{r \mid r \text{ is target of some } e \in D \wedge s(r) = 0\}$ be the set of roots. Furthermore, set $E_r := \{e \in D \mid r \text{ is target of e}\}$, $r \in R$. Then $E = \bigcup_{r \in R} E_r$ and E_r induces a contraction kernel C_r for any $r \in R$. It remains to show that the C_r are vertex disjoint. Assume the opposite, i.e. there exists a vertex u contained in C_v and in C_w for some $v \neq w \in R$. From (a) it follows that $u \notin \{v, w\}$. Hence, there exist edges $(u, v), (u, w) \in D$, a contradiction to $s(u) < 2$.

ii) (b) $\Rightarrow$ (a): Let T be the set of roots of the vertex disjoint contraction kernels and let C_t denote the unique contraction kernel with root t, $t \in T$. Furthermore, let $v \in G_D$. Since the C_t are vertex disjoint, exactly one of the following holds:

1. $v \in T$ and $s(v) = 0$.
2. $v \notin T$ and $s(v) = 1, t(v) = 0$.

Examples of kernels which do not fulfill the Definition 1 are shown in Figure 4(c1) where $s(v) = 1$ and $t(v) = 1$; and (c2) where $s(v) = 0$ and $t(v) = 2$. From the example in Figure 4(d) it is clear that only one edge can be contracted (otherwise one ends with forbidden contraction kernels), which means in general, vertex reduction factor can get arbitrarily close to 1.0.

Note that, in contrast to MIS, the roots of two contraction kernels may be neighbors. Condition (a) in Proposition 1 is fulfilled, if and only if no pair of directed edges from D belongs to the same $N(e)$, $e \in D$, where $N(e)$ is defined

in Definition 3. Hence, a maximal vertex disjoint union of contraction kernels may be found via a maximal set of directed edges that are independent with respect to $N(e)$. A parallel algorithm to find a maximal independent set with respect to $N(e)$ is specified in the next section.

Definition 3. *Let $e = (u, v)$ be a directed edge of G. Then the directed neighborhood $N(e)$ is given by all directed edges $e' = (u', v')$ such that*

$$u \in \{u'\} \cup \{v'\} \vee u' = v.$$

Neighborhood $N(e)$ of e is given by edges which point toward the source of e, edges with the same source u as e and the edges the source of which is the target of e. Note that edges pointing towards the target of e are not part of the directed neighborhood. Figure 4(e) depicts $N(e)$ in case of u and v both having 4 neighbors.

3.1 Maximal Independent Directed Edge Set Algorithm (MIDES)

To find a maximal (independent) set of directed edges (MIDES) forming vertex disjoint rooted trees of depth zero or one, we proceed analogously to the generation of maximal independent vertex sets (MIS), as explained in the Section 2. Let E_k denote the set of bi-directed edges in the graph G_k of the graph pyramid. We proceed as follows.

Algorithm 2 – MIDES Algorithm

1: Mark every directed edge e of E_k as *candidate*.
2: **while** there are candidates **do**
3: Assign random numbers to the candidates of E_k.
4: Determine the candidates e whose random numbers are larger than the random numbers of all candidates in its directed neighborhood $N(e) \setminus \{e\}$ and mark them as *member* (of a contraction kernel) and as *non-candidate*. Also mark every $e' \in N(e)$ of every new member e as *non-candidate*.
5: **end while**

Since the direction of edges uniquely determines the roots of the contraction kernels (the survivors), all the vertices which are the sources of directed edges are marked as non-survivor. An example of a set of contraction kernels C found by MIDES is given in Figure 4(f) (the survivors are depicted with black and non-survivors with white).

3.2 Experiments with Maximal Independent Directed Edge Sets

The same set of 1000 graphs (Section 2.2) was used to test MIDES. The numbers of levels needed to reduce the graph on the base level to an apex of the pyramid are shown in Figure 3 (c),(d). Again the vertical axis indicates the number of

Table 2. Reduction factors of vertices and edges.

Process	$\frac{\lvert V_k\rvert}{\lvert V_{k+1}\rvert}$ μ	σ	$\frac{\lvert E_k\rvert}{\lvert E_{k+1}\rvert}$ μ	σ
MIS	1.94	1.49	1.78	0.69
MIES	2.27	0.21	2.57	1.21
MIDES	2.62	0.36	3.09	1.41

vertices in the levels indicated by the horizontal axis. The experiments show that the **reduction factor** of MIDES is indeed **higher** than 2.0 (indicated by the dashed line in Figure 3(c),(d), even in the worst case (see [8] for details on numerical results). Also the *in-degrees* of the vertices is much smaller than for MIS (*max-degree* column in Table 1). For the case of the graph with size 200×200 vertices, MIDES needs less levels than MIS and MIES and the number of iterations needed to complete the maximal independent set was comparable with the one of MIS (Table 1, *correction* column). In Table 2, statistics of reduction factors for vertices ($|V_k|/|V_{k+1}|$) and edges ($|E_k|/|E_{k+1}|$) are given. From this table one can read that **MIDES** algorithm shows a **better reduction factor** than MIES [7] and MIS.

To summarize, in our experiments the reduction factor is always **higher** than 2.0 (outperforming MIS and MIES), even though the theoretical lower bound is 1.0.

4 Conclusion and Outlook

Experiments with (stochastic) irregular image pyramids using maximal independent vertex sets (MIS) showed that the reduction factor can get arbitrarily close to 1.0 for large images. After an initial phase of strong reduction, the reduction decreases dramatically. This is due to the evolution of larger and larger variations between the vertex degrees in the contracted graphs. To overcome this problem we proposed a new method (MIDES). Experimentally, this method has a reduction factor larger than 2.0. Moreover, MIDES, in contrast to MIES, allows us to take into account constraints on the directions of the contractions.

References

1. M. Bister, J. Cornelis, and A. Rosenfeld. A critical view of pyramid segmentation algorithms. *Pattern Recognition Letters*, Vol. 11(No. 9):pp. 605–617, September 1990.
2. M. Borowy and J. Jolion. A pyramidal framework for fast feature detection. In *Proc. of 4th Int. Workshop on Parellel Image Analysis*, pages 193–202, 1995.
3. M. Burge and W. G. Kropatsch. Run Graphs and MLPP Graphs in Line Image Encoding. In W. G. Kropatsch and J.-M. Jolion, editors, *2nd IAPR-TC-15 Workshop*

on Graph-based Representation, pages 11–19. OCG-Schriftenreihe, Österreichische Computer Gesellschaft, 1999. Band 126.

4. K. Cho and P. Meer. Image Segmentation from Consensus Information. *CVGIP: Image Understanding*, 68 (1):72–89, 1997.
5. N. Christofides. *Graph Theory - An Algorithmic Approach*. Academic Press, New York, London, San Francisco, 1975.
6. R. Glantz, R. Englert, and W. G. Kropatsch. Representation of Image Structure by a Pair of Dual Graphs. In W. G. Kropatsch and J.-M. Jolion, editors, *2nd IAPR-TC-15 Workshop on Graph-based Representation*, pages 155–163. OCG-Schriftenreihe, Österreichische Computer Gesellschaft, 1999. Band 126.
7. Y. Haxhimusa, R. Glantz, M. Saib, Langs, and W. G. Kropatsch. Logarithmic Tapering Graph Pyramid. In L. van Gool, editor, *Proceedings of 24th DAGM Symposium*, pages 117–124, Swiss, 2002. Springer Verlag LNCS 2449.
8. Y. Haxhimusa and W. G. Kropatsch. Experimental Results of MIS, MIES, MIDES and D3P. Technical Report No.78, PRIP, Vienna University of Technology. http://www.prip.tuwien.ac.at/ftp/pub/publications/trs, 2003.
9. J.-M. Jolion. Stochastic pyramid revisited. *Pattern Recognition Letters*, 24(8):pp. 1035–1042, 2003.
10. J.-M. Jolion and A. Montanvert. The adaptive pyramid, a framework for 2D image analysis. *Computer Vision, Graphics, and Image Processing: Image Understanding*, 55(3):pp.339–348, May 1992.
11. J.-M. Jolion and A. Rosenfeld. *A Pyramid Framework for Early Vision*. Kluwer Academic Publishers, 1994.
12. P. Kammerer and R. Glantz. Using Graphs for Segmenting Crosshatched Brush Strokes. In J.-M. Jolion, W. G. Kropatsch, and M. Vento, editors, *3nd IAPR-TC-15 Workshop on Graph-based Representation*, pages 74–83. CUEN, 2001.
13. W. G. Kropatsch. Building Irregular Pyramids by Dual Graph Contraction. *IEE-Proc. Vision, Image and Signal Processing*, Vol. 142(No. 6):pp. 366–374, December 1995.
14. W. G. Kropatsch and M. Burge. Minimizing the Topological Structure of Line Images. In A. Amin, D. Dori, P. Pudil, and H. Freeman, editors, *Advances in Pattern Recognition, Joint IAPR International Workshops SSPR'98 and SPR'98*, volume Vol. 1451 of *Lecture Notes in Computer Science*, pages 149–158, Sydney, Australia, August 1998. Springer, Berlin Heidelberg, New York.
15. W. G. Kropatsch and H. Macho. Finding the structure of connected components using dual irregular pyramids. In *Cinquième Colloque DGCI*, pages 147–158. LLAIC1, Université d'Auvergne, ISBN 2-87663-040-0, September 1995.
16. C. Mathieu, I. E. Magnin, and C. Baldy-Porcher. Optimal stochastic pyramid: segmentation of MRI data. *Proc. Med. Imaging VI: Image Processing*, SPIE Vol.1652:pp.14–22, Feb. 1992.
17. P. Meer. Stochastic image pyramids. *Computer Vision, Graphics, and Image Processing*, Vol. 45(No. 3):pp.269–294, March 1989.
18. P. Meer, D. Mintz, A. Montanvert, and A. Rosenfeld. Consensus vision. In *AAAI-90 Workshop on Qualitative Vision*, Boston, Massachusetts, USA, July 29 1990.
19. A. Montanvert, P. Meer, and A. Rosenfeld. Hierarchical image analysis using irregular tesselations. *IEEE Transactions on Pattern Analysis and Machine Intelligence*, PAMI-13(No.4):pp.307–316, April 1991.
20. A. Rosenfeld, editor. *Multiresolution Image Processing and Analysis*. Springer, Berlin, 1984.